Fuel 139 (2015) 441–456

Contents lists available at ScienceDirect

Fuel

journal homepage: www.elsevier.com/locate/fuel

Simulation and life cycle assessment of biofuel production via fast pyrolysis and hydroupgrading

Jens F. Peters [a], Diego Iribarren [a,*], Javier Dufour [a,b]

[a] Systems Analysis Unit, Instituto IMDEA Energía, Móstoles 28935, Spain
[b] Department of Chemical and Energy Technology, Rey Juan Carlos University, Móstoles 28933, Spain

HIGHLIGHTS

- Biomass fast pyrolysis and bio-oil hydroupgrading are simulated in Aspen Plus®.
- Bio-oil and synfuels are modeled with high level of detail (83 model compounds).
- Life cycle assessment is carried out based on simulation results.
- Electricity consumption is identified as a key source of environmental impacts.
- Greenhouse gas savings are 54.5% compared to the equivalent fossil fuel.

ARTICLE INFO

Article history:
Received 30 June 2014
Received in revised form 27 August 2014
Accepted 3 September 2014
Available online 16 September 2014

Keywords:
Biofuel
Biorefinery
Fast pyrolysis
Life cycle assessment
Process simulation

ABSTRACT

A biofuel process chain based on fast pyrolysis of hybrid poplar and subsequent hydroupgrading of the obtained bio-oil is simulated using Aspen Plus®. The simulation includes the pyrolysis plant and the biorefinery with its hydrotreating, hydrocracking, distillation and steam reforming sections. All parts of the process are modeled with a high level of detail, using 83 model compounds and a kinetic reaction model for the pyrolysis plant. A cross-check with published experimental data is included in order to validate the model. Based on the simulation results, a Life Cycle Assessment (LCA) is conducted for the biofuel products, identifying the processes with the highest contribution to the environmental impacts. The obtained synthetic biofuels are compared with their fossil fuel equivalents in order to quantify their potential environmental benefits. LCA results show greenhouse gas (GHG) savings of 54.5% for the produced fuel mix compared to conventional gasoline and diesel. Electricity consumption is one of the keys for reducing the overall environmental impact, while GHG savings could be enhanced by improving the thermal efficiency of the combustion processes in the plants. The biofuel pathway assessed is found to be an interesting option to produce second-generation biofuels with optimization potential in all phases of the system.

© 2014 Elsevier Ltd. All rights reserved.

1. Introduction

As reflected in the EU Renewable Energy Directive 2009/28 (RED) [1], biofuels are considered one of the keys to reduce greenhouse gas (GHG) emissions as well as the high dependency of the European transport sector on imported fossil oil. For 2020, a 10% share of renewable energy is set as a target for the transport sector. This target is not without controversy, as first generation ethanol and biodiesel, which make up virtually all of the current biofuel mix, often show relatively low GHG savings and significant other environmental impacts [2–6]. The proposal for amending the RED in this regard [7] limits the contribution of conventional biofuels to 5% of the final energy consumption in transport, expecting this gap to be filled by second-generation biofuels. These can be produced from non-food crops on unused agricultural land at high yields while requiring little agricultural inputs. Poplar and willow from short-rotation cultivation and perennial grasses like miscanthus or switchgrass are among the most promising energy crops of this type [8].

One of the most efficient options to produce biofuels from this lignocellulosic biomass is its thermochemical conversion by fast pyrolysis [9–14]. The obtained pyrolysis oil (or bio-oil) is a liquid of high density and moderate heating value that can be upgraded in a biorefinery to gasoline and diesel blendstocks [15–17]. Pyrolysis-based biofuels have a high potential for reducing the

* Corresponding author. Tel.: +34 91 737 11 19.
E-mail address: diego.iribarren@imdea.org (D. Iribarren).

http://dx.doi.org/10.1016/j.fuel.2014.09.014
0016-2361/© 2014 Elsevier Ltd. All rights reserved.

carbon emissions of the transport sector. Potential GHG savings of 60–88% compared to fossil fuels are reported in the literature [18–21]. Nevertheless, in order to provide a comprehensive picture of the environmental performance of biofuel systems, the assessment should not be limited to GHG emissions. Life Cycle Assessment (LCA) is a helpful tool for this purpose, as it comprehensively assesses the impacts of a process or product for a whole set of impact categories [22].

LCA is a standardized methodology [23,24] frequently applied to biofuel systems, mainly to bioethanol and biodiesel processes [25–27]. Nevertheless, only a few works dealing with the LCA of pyrolysis-based biofuels have been published so far [18,20,21,28–31] and there is a lack of detailed inventory data for further studies. This may be partially due to the very limited amount of commercial-scale pyrolysis installations being operative to date [32]. Hence, inventory data are difficult to obtain and assessments have to be based on process simulation. The reference works in this field are the techno-economic studies by Ringer et al. [33], Jones et al. [34] (both based on wood chips as feedstock), and Wright et al. [35] (using corn stover as feedstock), who developed detailed simulations of a complete biofuel process chain [33–36]. Nevertheless, they use black box approaches for modeling the pyrolysis reaction mechanisms and a limited number of model compounds, thus resulting in a considerable simplification of the process. Existing LCA studies on pyrolysis biofuels are usually based on these works, either exclusively [20,21,28,29] or with some modifications according to data retrieved from other literature sources [18,30,31].

In this study, an innovative Aspen Plus® [37] simulation of a typical pyrolysis and hydrotreating process chain is presented. Within the simulation, a novel kinetic reaction model is used for calculating pyrolysis products based on the atomic and biochemical composition of the lignocellulosic biomass feedstock. In contrast to previous simulation approaches, this leads to a predictive calculation of the pyrolysis products for any lignocellulosic feedstock as well as to a very detailed modeling of the bio-oil, using 33 model compounds. The simulation results are verified against existing experimental data and used as a source of detailed inventory data. According to these results, the life-cycle performance of the produced biofuels is evaluated and compared with that of conventional fossil fuels.

2. Materials and methods

The goal of this study is to evaluate the environmental performance of synthetic biofuels produced via pyrolysis. Bio-oil is obtained through fast pyrolysis of a lignocellulosic feedstock and then upgraded in a biorefinery to synthetic fuels. The pyrolysis plant and the biorefinery are simulated in Aspen Plus® in order to obtain detailed inventory data. The environmental performance of the biofuels is evaluated following an attributional LCA approach. In attributional LCAs, the assessed system is treated like an isolated process that does not interact with global markets. Attributional LCA gives therefore a picture of the impacts directly associated with the life cycle of a product, but it is not suitable for assessing consequences of e.g. policy decisions. In contrast, consequential LCA takes into account the market effects of the production and consumption of a product. This requires explicit modeling of market mechanisms, making the assessment more comprehensive but much more complex and associated with additional uncertainties [38].

2.1. LCA framework

The system boundaries are set according to Fig. 1, including the whole conversion process from feedstock production to the produced biofuels at the refinery gate. Capital goods are not included, assuming that their influence on the final LCA results is negligible [27,39]. Moreover, this assumption facilitates comparison with other studies in this field [18,20,21,28]. Production is assumed to be located in central Spain, one of the countries with the highest agricultural bioenergy potential in Europe [8]. Hence, data specific for Spain are used for all secondary data (electricity mix, average vehicle, etc.) when available.

The functional unit (FU) used in this work is 1 MJ of energy content of the obtained synthetic biofuel mix (gasoline and diesel). This is a common FU for biofuel assessment [20,21,27,40] and allows for comparing the results with the GHG saving targets stated in the RED [1]. According to the lower heating value (LHV) of the fuels and the production rates taken from the simulation results, this corresponds to 0.51 MJ of gasoline and 0.49 MJ of diesel.

The assessed processes are multifunctional, producing more than one product. Allocation is used to deal with this situation. Since all products have energetic uses, allocation is carried out according to their energy content (LHV basis). This is also in accordance with the RED methodology, which defines energy allocation on an LHV basis as the methodology for distributing the GHG emissions in multifunctional systems [1].

In addition to the bio-oil, the pyrolysis reactor yields char as a by-product. Since the char is not further processed to synthetic fuels in the biorefinery and constitutes an independent product, a share of the environmental impacts caused by the pyrolysis process has to be allocated to the char. This allocation is calculated based on the mass flows and the heating values of the bio-oil and char products leaving the plant. The corresponding allocation percentages are presented in Table 1 ('Pyrolysis').

In the biorefinery, synthetic gasoline and diesel are produced plus process steam generated by cooling the hydrotreating reactors. Similarly to the char in the pyrolysis plant, this steam is a by-product that does not contribute to the production of the synthetic fuels. It is assumed that this steam constitutes a valuable by-product for use in neighboring industrial facilities. Therefore, allocation is done according to the energy content of the products as obtained from the simulation. The corresponding allocation percentages are given in Table 1 ('Biorefinery').

2.2. System description

The system subject to assessment produces biofuels by fast pyrolysis of poplar from hypothetical short-rotation plantations in central Spain. Spain is the country with the third highest agricultural bioenergy potential in the EU-27 and poplar is one of the most suitable energy crops for deployment in this region [8,41]. Biomass is a local resource and small-scale pyrolysis plants are assumed to be located close to the plantation sites for minimizing transport distances [42,43], while the biorefinery is assumed to be part of an existing refinery installation due to economic reasons [34,44]. This decentralized biorefinery configuration has been found to be environmentally more favorable than an integrated pyrolysis/biorefinery configuration in a previous screening assessment comparing different bio-oil use options [45].

For the analysis, the whole system is divided into subsystems. According to Fig. 1, these include agriculture and cropping, biomass transport, the pyrolysis plant, bio-oil transport and the biorefinery plant. The pyrolysis plant and the biorefinery are modeled in Aspen Plus® (shaded grey in Fig. 1), while data for the remaining processes are retrieved from the literature and the ecoinvent database version 2.2 [46–49].

2.2.1. Agriculture and cropping

The agricultural inputs required for poplar short-rotation cultivation (e.g., pesticides and fertilizers) are taken from the literature

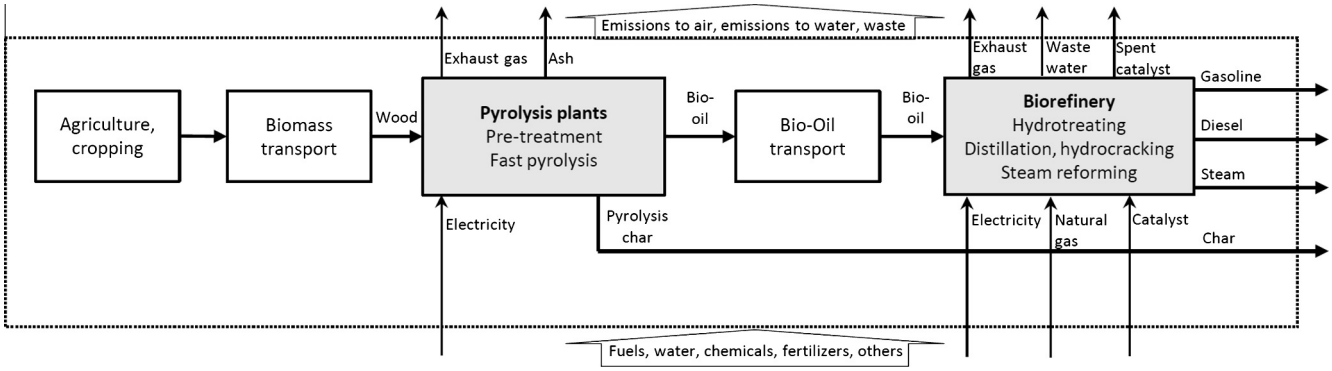

Fig. 1. Block diagram of the biofuel system.

Table 1
Energy-based allocation percentages for the pyrolysis and the biorefinery sections.

Item	Amount per FU	Unit	LHV (MJ kg^{-1})	Allocation percentage (%)
Pyrolysis				
Bio-oil	6.03E−02	kg	16.00	87.07
Char	5.73E−03	kg	24.48	12.93
				100
Biorefinery				
Gasoline	0.510	MJ	42.01	47.77
Diesel	0.490	MJ	42.25	45.81
Process steam	0.019	kW h	–	6.42
				100

[50,51]. The fertilizer needs are then corrected by the calculated nutrient uptake for the supposed yield. The nutrient (N, P, K) uptake during biomass growth is estimated based on the atomic composition and the ash content of the poplar biomass according to Gasol et al. [51] and the average nutrient content of the ash taken from the Phyllis database [52]. The fertilizer demand is then calculated by multiplying the nutrient uptake with the assumed yield of 13.5 t ha^{-1} [50,53,54] for an irrigated poplar plantation located in Spain, and the fertilizer application rates taken from Gasol et al. [51] are modified accordingly.

Nutrient leaching and emissions (N_2O, ammonia, NO_x) due to the application of fertilizers are calculated for N and P_2O_5 according to the methodology given in the ecoinvent report [55]. For N-fertilizer application, the N-leaching correction factors for Spanish conditions are applied. Regarding irrigation water, a value of the upper end within the range given by Gasol et al. [51] is used, as the experimental plot used by them was located in a region with higher average rainfall than that of the assumed location in central Spain.

Land use change implies changes of the carbon stock stored in the soil as organic matter. In the given case, fallow agricultural land is assumed to be used for cultivation of the short-rotation crops. Soil carbon stock is calculated according to the methodology given by the Intergovernmental Panel on Climate Change (IPCC) [56–58] for a location in central Spain. According to the IPCC Tier 1 methodology, the given plantation can be considered grassland with two improvements due to fertilization and irrigation and it gives an increase of C stock of 10.09 t C ha^{-1} compared to fallow land. The main inventory data of the agricultural phase are summarized in Table A1 in Appendix.

2.2.2. Biomass transport

The pyrolysis plants (with a capacity of 11 t h^{-1} of wet feedstock and 7000 h of annual operation) require 38,500 t y^{-1} of dry feedstock. Five plants are needed in order to provide the bio-oil required by a biorefinery processing 20 t h^{-1} of bio-oil. With yields of 13.5 t ha^{-1} (dry basis) [51], this requires 3000 ha of plantation for each pyrolysis plant. Furthermore, an average 2% land availability for short-rotation plantations is used as the plants are normally situated close to the plantations. Assuming a circular shape, the corresponding collecting area is 44 km in diameter and the average transport distances of the biomass to the pyrolysis plants is 15.5 km, using the calculation method given by Gasol et al. [50]. Storage of the harvested wood chips takes place at the plantation site without any drying (an average 50% moisture as delivered to the plant is therefore assumed) and then the biomass is shipped to the plant site by truck just in time. Possible natural drying on the site during open air storage is not taken into account. Decomposition effects, which would reduce the energy content with storage time, are also excluded [59].

2.2.3. Pyrolysis plant

In the pyrolysis plant, the biomass is pre-treated and converted by fast pyrolysis into bio-oil, gas and char. The gas fraction and part of the char are burned on site for process heat generation. As the pyrolysis plant is simulated in Aspen Plus®, it is treated in detail in Section 3.1.

2.2.4. Bio-oil transport

An average transport distance of 200 km is assumed from the pyrolysis plants to the biorefinery. This accounts for the fact that the biorefinery is located close to an existing refinery installation and hence not in the proximity of the plantations. The use of local feedstock is assumed and no imports are considered.

2.2.5. Biorefinery

In the biorefinery, the raw bio-oil is converted via hydroupgrading into gasoline and diesel blendstocks. The biorefinery consists of

three principal processing steps: hydrotreatment, product separation (including hydrocracking), and steam reforming. It is described in detail in Section 3.2. Annual operating times are 7000 h for the upgrading process in the biorefinery. The biorefinery is assumed to be included in an existing refinery due to economic reasons. Hence, handling and transport of the pyrolysis-based fuels are the same as for their fossil equivalents. The comparison with the equivalent fossil fuels can consequently be made at the refinery gate and the downstream transport processes do not have to be accounted for.

3. Process simulation

3.1. Pyrolysis plant

The pyrolysis plant converts the raw biomass into bio-oil and a char by-product. The simplified Aspen Plus® flowsheet of the pyrolysis plant is shown in Fig. 2, while detailed stream data can be found in Tables A2 and A3 in Appendix.

Pre-treatment. Moist biomass (BIOM-WET in Fig. 2; represented by a non-conventional component in Aspen Plus®) is dried in a direct-contact dryer (PY-DRYER) using the hot exhaust gases (DRYINGAS) from the gas and char combustor (GASCOMB). The amount of air fed to the combustor is controlled by a design specification in order to maintain an exhaust gas flow sufficiently high as to dry the biomass to the desired 7% water content. A grinder followed by a sieve (PY-MILL) reduces the particle size to 3 mm, as required by circulating fluidized bed reactors [60]. For the required grinding work an average value in accordance with published literature is used [34,61]. Except for the mill, electricity consumption for biomass handling is not taken into account.

Pyrolysis reactor. The dry and ground biomass (BIOMFEED) enters the pyrolysis reactor (PY-REACT) where it is decomposed under fast pyrolysis conditions into bio-oil, gas and char. Typical conditions in a circulating fluidized bed reactor are considered [34]: 520 °C, 2 s bed residence time, 0.5 s vapor residence time, and a gas-to-feed ratio for bed fluidization of 1.0 on a weight basis. The pyrolysis reactor is based on a kinetic reaction model with over 150 individual decomposition reactions implemented. This permits a predictive calculation of the pyrolysis products according to feedstock composition and reactor conditions. The final and intermediate pyrolysis products are modeled with a high level of detail; the bio-oil is composed of up to 31 model compounds, and the char is modeled as a non-conventional component with realistic O, H, N, S and Cl content. Release mechanisms of these elements are included and the corresponding contaminant formation is simulated. More details about the reaction model are published in a previous work [62]. Heat for the reactor is provided by the combustor (GASCOMB).

Product recovery. The pyrolysis products that leave the reactor (PYR-OUT) pass a series of cyclones to separate the char, and the remaining vapors are then quenched with cold bio-oil (QENCHLIQ) to stop the secondary decomposition reactions. A water cooler further reduces the temperature of the product stream in order to maximize the liquid recovery in the subsequent flash unit (PY-FLASH), where the produced gases are separated from the condensable fraction. Virtually all alkali metals and contaminants contained in the biomass are retained in the char, with the exception of Cd, for which a temperature dependency exists, with ca. 50% being transferred to the oil at pyrolysis temperatures around 500 °C [63–66]. The part of the recovered liquid that is not recirculated to the quench cooler leaves the pyrolysis plant as bio-oil product (BIOOIL).

Gas and char combustor. A share of the gas fraction is recirculated to the pyrolysis reactor for fluidizing the reactor bed (FLUEGAS), while the remaining part (PRODGAS) is burned in the combustor (GASCOMB). As burning the pyrolysis gases does not provide sufficient heat for the pyrolysis reactor and for drying the biomass, a fraction of the pyrolysis char has to be burned additionally. The char separated in the cyclone is split into a product fraction (CHARPROD) and a fuel fraction (CHARCOMB). The former is quenched with water in order to avoid auto-ignition, while the latter is burned with the gases in the GASCOMB. As the exhaust gases from the combustor are used for drying the biomass (DRYINGAS), the biomass dryer determines the exhaust gas flow and the air flow to the combustor (COMBAIR). For the wet poplar feedstock, the dryer requires significant amounts of heat and the combustion takes place with excess air >20%. The combustor works at pressures of 1.6 bar, required for overcoming the pressure drops in the downstream components such as the dryer. A cyclone separates the ashes (ASHOUT) from the exhaust gases before recirculating them to the dryer.

3.2. Biorefinery

3.2.1. Hydrotreatment

A two-stage catalytic hydrotreatment (Fig. 3) converts the bio-oil into an almost oxygen-free hydrocarbon product, modeled by

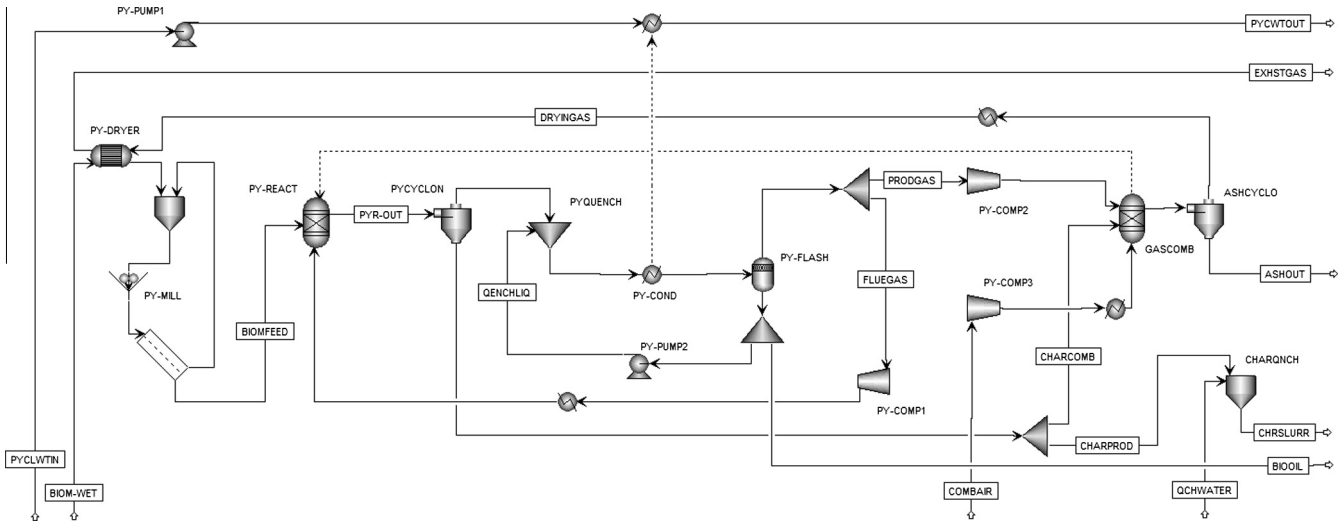

Fig. 2. Simplified Aspen Plus® flowsheet of the pyrolysis plant.

up to 52 model compounds with C4–C18 chain length, including alkanes, naphthenes, mono- and poly-aromatics, furans, phenols and alcohols. The catalysts used in the hydrotreating reactors are commercial Co–Mo catalysts [17,34]. Detailed stream data can be found in Table A4 in Appendix.

The bio-oil from the pyrolysis plant (BIOOIL) and hydrogen (HTH2FEED) are pressurized up to 170 bar and fed to the first reactor (HTREACT1). In this reactor, operating at 270 °C, the bio-oil is stabilized for its further processing (oxygen content of the intermediate product around 30%) [15,17,67]. In the second hydrotreating reactor (HTREACT2) the stabilized oil (HT1OUT) is deoxygenated to <2% oxygen content under more severe conditions (150 bar, 350 °C) [15,17,67]. Both reactors are modeled as RYield reactors and use an iterative linear regression algorithm to adjust an initial product distribution based on literature data [16,17,68,69] to the actual feed composition. Afterwards, the product (HT2OUT) is cooled and the aqueous fraction (HTAQUOUS) is separated from the organic fraction (HTORGANC) in a high-pressure flash unit (HT-FLASH). The aqueous fraction contains around 1% organics, mainly alcohols and phenols. As the hydrocracking reactions are highly exothermic, a significant amount of steam can be produced by cooling the reactors (STEAMHOT). For cooling the hydrotreater products and condensing the water before the high-pressure flash unit, a cooling water circuit (HTCLWTIN and HTCLWOUT) is required.

The consumption of catalyst in the hydrotreaters cannot be simulated in Aspen Plus®, and literature data on catalyst poisoning in bio-oil hydrotreaters are not available. Therefore, data for hydrotreaters in petroleum refineries are used. The range of catalyst consumption found in literature is 0.05–0.15 kg per metric ton of feedstock [70–73], with the lower end value used for this study. The catalyst contains 11% Mo, 4% Co and 7% S on an Al_2O_3 support [74,75].

3.2.2. Distillation and hydrocracking

Distillation. The dewatered, organic fraction from the hydrotreatment is separated into its fuel fractions by distillation, while the remaining heavy bottom stream is converted into lighter products via hydrocracking (Fig. 4). The organic fraction from the hydrotreating section (HTORGANC) contains a significant amount of unreacted hydrogen. In order to separate this hydrogen before sending the stream to the distillation columns, a pre-flash unit is required, splitting the feed stream into a gas fraction (FLSHGAS) and a liquid fraction that goes to the distillation process (DISTFEED). In the first distillation column (DISTILL1), operating with eight stages and under atmospheric pressure, the gasoline fraction (GASLNOUT) is separated from the heavier fraction (D1BOTTOM). A small gas fraction is also produced (DISTGAS), which cannot be condensed under non-cryogenic conditions. The bottom stream enters the second column (DISTILL2), operating with nine stages and under vacuum, separating the diesel fraction (DIESLOUT) from the heavier fraction (D2BOTTOM).

Hydrocracking. The heavy fraction, represented in the simulation by chrysene, is pressurized and mixed with hydrogen (HCH2FEED) before being fed to the hydrocracker (HCRACKER), which splits up the heavy hydrocarbons into smaller molecules under catalyst influence and severe reactor conditions (670 °C, 90 bar, commercial Ni catalyst) [34]. The hydrocracker is modeled as an RStoic reactor where a hypothetical reaction stoichiometry is implemented based on literature data [69]. The product stream (HCRCKOUT) is de-pressurized, cooled and recirculated to be mixed with the organic fraction from the hydrotreating section (HTORGANC). A cooling water circuit (HCCLWTIN and HCCLWOUT) is required for the condensers of the distillation columns. Heat for the reboilers is obtained from the steam produced in the hydrotreating section and from the combustor in the steam reforming section (not shown in Fig. 4). The detailed stream data for the distillation and hydrotreating section can be found in Table A5 in Appendix.

3.2.3. Steam reforming

The hydrogen required by the hydrotreaters and the hydrocracker is produced by a steam reforming process using the light hydrocarbons contained in the gas streams from the distillation section (FLSHGAS and DISTGAS). A simplified flowsheet of the steam reforming process is shown in Fig. 5, while Table A6 in Appendix summarizes the main stream data. To satisfy the overall process hydrogen demand, additional natural gas (SRCH4EXT) must be provided to the reactor.

Steam reforming. The gases from the pre-flash unit in the distillation section (FLSHGAS) are split, according to the fuel

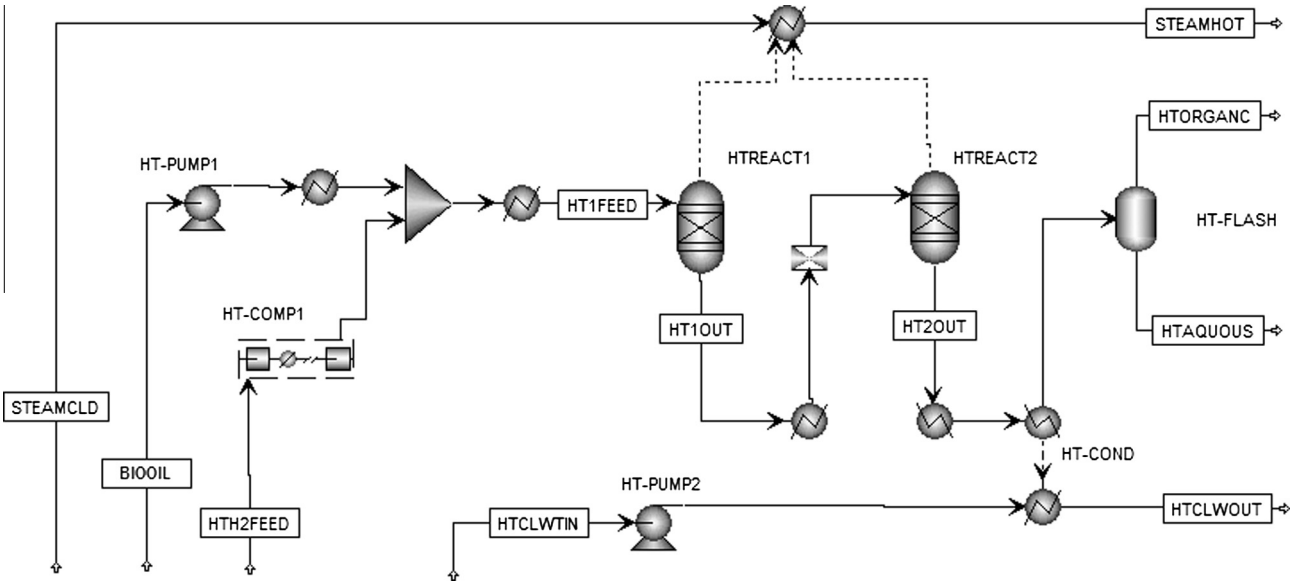

Fig. 3. Simplified Aspen Plus® flowsheet of the hydrotreating section.

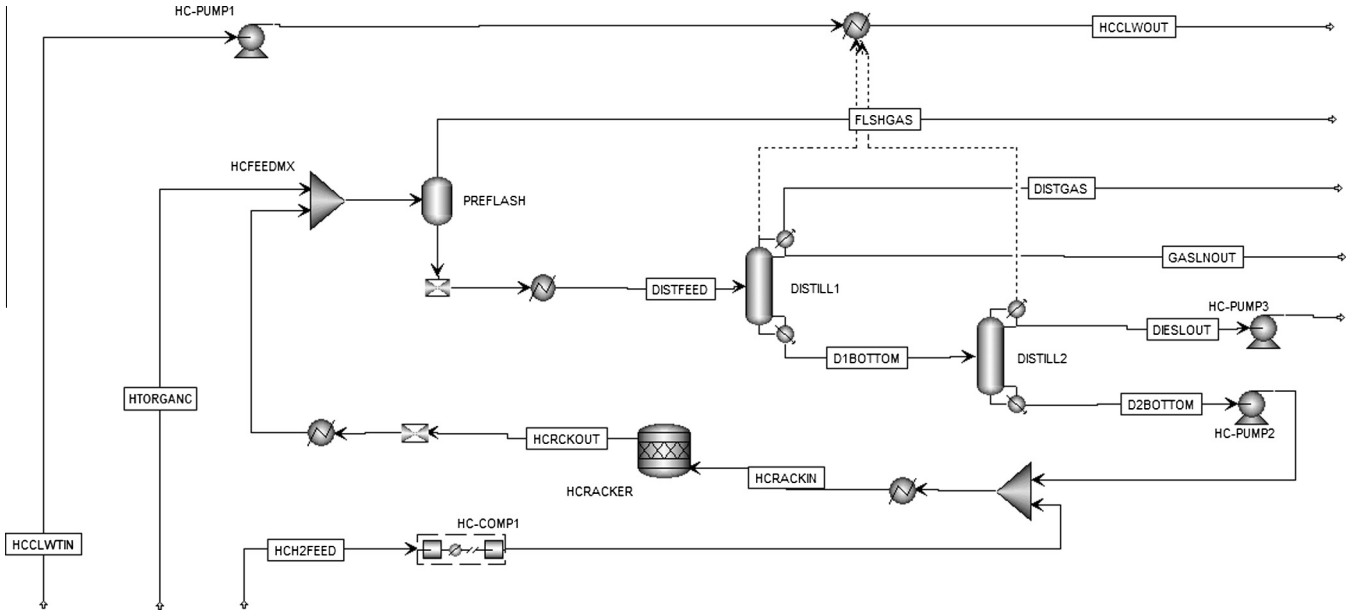

Fig. 4. Simplified Aspen Plus® flowsheet of the distillation and hydrocracking section.

requirements of the combustor (SROFGCMB), into a fraction for reforming (SRGASRCT) and a fraction for direct combustion. The gas fraction for reforming is mixed with water (SRAQUIN) and the required amount of natural gas (SRCH4EXT), heated and fed to the steam reforming reactor (SRREACT). The steam reformer is modeled as an RGibbs reactor that calculates the reaction products by Gibbs free energy minimization under the given reactor conditions. A reforming temperature of 950 °C gives the best results for the composition of the gas feed, containing a high share of non-methane gases.

Water gas shift. The reactor product stream (SRRCTOUT) is cooled down and enters the water gas shift reactor (WGSREACT), modeled as an REquil reactor that calculates the products of the water gas shift reaction by Gibbs free energy minimization. It operates under 350 °C and increases the amount of hydrogen produced by converting CO and water to CO_2 and H_2. The product stream (SRWGSOUT) is cooled and flashed (SRFLASH), separating the water fraction from the gases. A PSA unit (SRPSA; modeled by a user-defined splitter) separates about 90% of the hydrogen from the product gases, which is then delivered to the hydrotreaters (SRH2THDO) and the hydrocracker (SRH2THCR).

Combustor. The off-gas stream (SROFFGS1), containing mainly CO_2 and unreacted hydrocarbons, is mixed with the gas stream from the distillation column (DISTGAS), combustion air (SRCMBAIR) and the fraction separated from the flash gas stream (FLSHGAS) for direct combustion (SRCMBIN). In the combustor (SROFGCMB), the heat required by the steam reforming reactor is generated. Reaction products (SRCMBEXG) are calculated by Gibbs free energy minimization for a combustion temperature around 1100 °C. A share of the water condensed and separated in the SRFLASH is recirculated and fed to the steam reforming process, while the excess water leaves the plant as wastewater (SRLIQOUT). A steam-to-carbon ratio of 4.5 minimizes the requirements of natural gas for the given gas composition. A cooling water circuit (SRCLWTIN and SRCLWOUT) is required for condensing the aqueous fraction.

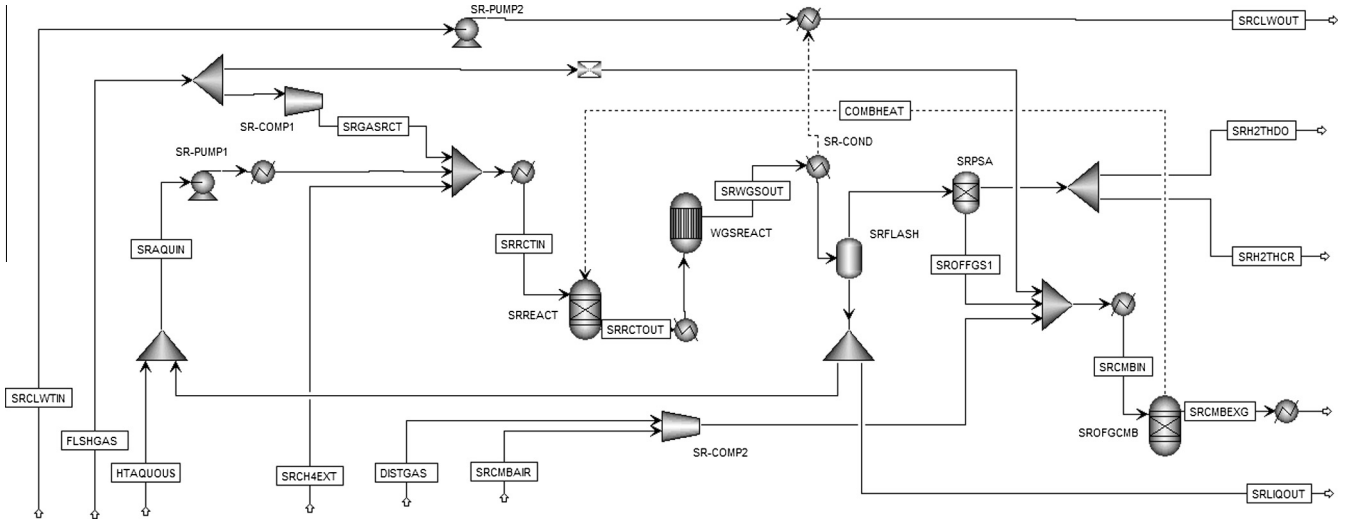

Fig. 5. Simplified Aspen Plus® flowsheet of the steam reforming section.

4. Results and discussion

4.1. Simulation results and validation

Pyrolysis plant. Due to the kinetic reaction model used for calculating the pyrolysis products, detailed information about reactor yields and product compositions are obtained from the simulation. The obtained yields are 68.8% bio-oil, 14.3% gas and 16.9% char, with the composition of the bio-oil presented in Table 2. 61% of the produced char is burned in the combustor of the plant for generating process heat and does not leave the plant, giving an effective char yield of 6.6%. The char product has an oxygen content of 13% and an LHV of 24.5 MJ kg^{-1}, while the bio-oil contains 41% oxygen and has an LHV of 16.0 MJ kg^{-1}. Further details can be found in the stream tables in Appendix (Tables A2 and A3).

Since these results are values calculated using a novel kinetic model, they are validated with published data. For a hybrid poplar feedstock, Jones et al. [34] report yields of 75% bio-oil, 12% gas and 13% char, and Ringer et al. [33] 73% bio-oil, 12% gas and 15% char. Hence, a high correlation of the simulation model with existing works is achieved in this respect.

When comparing the composition of the bio-oil product with published experimental work [76–78], good correlation is also found for most of the compounds. Oasmaa et al. [77] report yields of 25% water, 30% sugar-derived, 25% aldehydes and ketones, 17% degraded lignins and 3% others for eucalyptus wood under similar reactor conditions. These are values close to those obtained from the simulation, with a bio-oil of slightly higher water content. Furthermore, Dong et al. [76] report 12% sugar-derived (anhydrosugars and furans), 15% aldehydes, 6% ketones, 18% acids and 25% phenols and degraded lignin for the pyrolysis of poplar wood at 500 °C with 5 s residence time. When cross-checking against these values, good coincidence is observed for most of the fractions. Only the content of organic acids is significantly higher and the degraded sugars significantly lower than in the simulation. Nevertheless, it has to be taken into account that no final bio-oil yield is reported by Dong et al. [71] and that compounds could be identified for only 84% of the peak area of the gas chromatography analysis. The lower yields of degraded sugars reported in their work might be a result of the longer residence time, since at longer residence times the sugar-derived fraction (mainly levoglucosan and xylose) decomposes quickly. The higher hemicellulose content of the feedstock used in the experiments might be a factor further influencing the high yield of organic acids reported for the experiments, since these acids derive from the decomposition of hemicellulose.

Biorefinery. In the biorefinery, 0.96 MJ of bio-oil are consumed for producing 1.00 MJ of biosynfuels, though with a significant input of external energy, 0.27 MJ of natural gas and 0.04 MJ of electricity. In comparison with the study by Jones et al. [34], this is a slightly lower output of synthetic fuel per amount of bio-oil processed, but with lower requirements of auxiliary input.

Table 3 shows the final product yield and composition as obtained from the simulation. Literature with experimental data for hydrotreating products is scarce, but a few publications exist that give a typical distribution of the hydrotreating products for bio-oil from the fast pyrolysis of lignocellulosic feedstocks [16,17], with 54% of the liquid product within the gasoline range (33% naphthenes, 18% paraffins and 3% polynaphthenes and aromatics), 35% in the diesel range (11% aromatics and 24% (poly-) naphthenes and paraffins), and 11% heavy residue with a boiling temperature above 325 °C. The composition obtained from the simulation hence shows good correlation with the available experimental data.

Electricity consumption. Apart from the natural gas required by the steam reformer, electricity is the main external energy input to the process. The electricity consumption of the system is broken down by component in Table 4. The pyrolysis plant is responsible for 70% of the overall electricity needs of the system, with the combustion air compressor (PY-COMP3) as the main consumer. The high electricity demand of this compressor is a result of the high air flow entering the dryer (PY-DRYER) in combination with the relatively high operating pressure of the combustor. Both are directly related to the biomass dryer, which requires this high air flow and causes additional pressure drops. In the biorefinery, the hydrogen compressor of the hydrotreating section (HT-COMP1) shows the highest electricity demand, followed by the combustion air compressor (SR-COMP2) and the off-gas compressor (SR-COMP1) in the steam reforming section.

The simulation of the biofuel process chain is the key source of data for the environmental assessment of the synthetic biofuels produced (Section 4.2). The main direct inputs and outputs of the conversion processes are summarized in Table 5, while detailed stream tables can be found in Tables A2–A6 in Appendix.

4.2. LCA results

Four impact categories are considered for the environmental characterization of the system: abiotic depletion (ADP), acidification (AP), eutrophication (EP), and global warming potential (GWP). These are among the most common and well-

Table 2
Bio-oil composition obtained from the simulation of the fast pyrolysis of hybrid poplar biomass.

Oil composition	
Water	18.92%
Organic acids	4.68%
Phenols	0.25%
Aromatics	0.00%
Aldehydes	20.91%
Ketones	2.88%
PAH	0.76%
Sugar-derived	27.34%
Alcohols	3.47%
Lignin-derived	18.80%
Nitrogen content	1.98%
Oil ultimate analysis	
C	51.85%
H	6.79%
O	40.85%
N	0.51%

Table 3
Final product composition for the two-stage hydrotreating process according to simulation results.

Product	Compound group	Yield (%)
Gasoline	C_5–C_{10} paraffins	15.70
C_5–C_{12}	C_5–C_{10} naphthenes	31.08
	Polynaphthenes	0.00
	Benzenes, phenols	4.75
	(Total Gasoline)	51.53
Diesel	Propylbenzene, propylphenol	2.38
C_8–C_{18}	Naphthalene	1.06
	C_{11}–C_{18} (Poly-)naphthenes and paraffins	25.58
	(Total Diesel)	29.02
Heavies	Chrysene	14.28
	(Total Heavies)	14.28
Others	Furans	3.29
	Alcohols	1.88
	(Total others)	5.17

Table 4
Electricity consumption of the process chain broken down by component (values per MJ of synthetic fuel mix).

Pyrolysis	kW h	Contribution (pyrolysis) (%)	Contribution (overall) (%)
PY-MILL	3.78E−03	13.88	9.83
PY-COMP1	3.18E−03	11.67	8.27
PY-PUMP1	6.56E−05	0.24	0.17
PY-COMP2	2.66E−04	0.98	0.69
PY-COMP3	1.99E−02	73.00	51.70
PY-PUMP2	6.26E−05	0.23	0.16
Total	2.72E−02	100.00	70.82
Biorefinery	**kW h**	**Contribution (biorefinery) (%)**	**Contribution (overall) (%)**
HT-PUMP1	5.95E−04	5.30	1.55
HT-PUMP2	1.78E−05	0.16	0.05
HT-COMP1	4.83E−03	43.00	12.55
HC-COMP1	3.77E−04	3.36	0.98
HC-PUMP1	2.84E−05	0.25	0.07
HC-PUMP2	2.66E−05	0.24	0.07
HC-PUMP3	1.78E−06	0.02	0.00
SR-PUMP1	5.45E−05	0.49	0.14
SR-COMP1	2.02E−03	17.99	5.25
SR-COMP2	3.25E−03	28.94	8.45
SR-PUMP2	2.78E−05	0.25	0.07
Total	1.12E−02	100.00	29.18

established categories for assessing bioenergy systems in LCA studies [5,25,27]. They are evaluated according to the CML method [79]. Additionally, the cumulative non-renewable (fossil and nuclear) energy demand (CED_{nr}) of the system is quantified [80]. The software SimaPro is used for the computational implementation of the inventories [81].

4.2.1. Environmental characterization

The environmental impacts caused by the process chain are allocated to the two fuel products (gasoline and diesel) according to their energy content. Thus, the environmental profile obtained per MJ of fuel is the same for synthetic gasoline and diesel, as well as for the corresponding fuel mix. Table 6 shows the environmental characterization results for 1 MJ of synthetic biofuel.

The pyrolysis-based fuels (gasoline and diesel) show a negative GWP impact (Table 6). This is a result of the system boundary, which does not include the combustion of the fuels. The synthetic fuels hence act as virtual carbon sinks, with the carbon fixed during biomass growth being stored in the fuels. However, burning the fuels would release the equivalent amount of carbon and result in a positive GWP impact (the well-to-wheels GHG emissions, as discussed in Section 4.2.3). Principal contributors to GWP are the pyrolysis and the biorefinery plants.

The AP impact is caused mainly by the pyrolysis plants, while the agricultural phase is the main contributor to EP, as discussed in detail in Section 4.2.2. ADP is dominated by the biorefinery plant, which consumes significant amounts of natural gas for producing the hydrogen required by the hydrotreaters. Transport contributes only a minor share to all impact categories.

Similar to ADP, the CED_{nr} category is dominated by the biorefinery, which contributes ca. 44% to this category. The life-cycle energy balance (computed as the difference between the potential energy output and the CED_{nr} indicator) shows a favorable value of 0.13 MJ FU^{-1}. This indicates that the fuel energy output exceeds the corresponding non-renewable energy demand of the biofuel process chain, being electricity consumption and the fossil natural gas required by the biorefinery for hydrogen production the main inputs of non-renewable energy.

Table 5
Main inventory data (per MJ of synthetic fuel mix) for the conversion processes (pyrolysis and biorefinery).

Inputs			Outputs		
Item	Amount	Unit	Item	Amount	Unit
Pyrolysis			*Pyrolysis*		
Wood chips	0.16	kg	Products		
Electricity	2.72E−02	kW h	Char	5.73E−03	kg
Transport	5.06E−03	t km	Bio-oil	6.03E−02	kg
			Emissions to air		
			CO_2	4.27E−02	kg
			SO_2	2.37E−05	kg
			NO_x, as NO_2	3.55E−05	kg
			HCl	6.15E−06	kg
			Particulates	1.74E−06	kg
Biorefinery			*Biorefinery*		
Bio-oil	6.03E−02	kg	Products		
Natural gas	0.27	MJ	Syngasoline	0.51	MJ
Electricity	1.12E−02	kW h	Syndiesel	0.49	MJ
Catalyst	6.03E−06	kg	Steam	1.91E−02	kW h
Transport	2.41E−02	t km	Emissions to air		
			CO_2	5.69E−06	kg
			SO_2	2.27E−15	kg
			NO_x, as NO_2	4.60E−05	kg
			Waste to treatment		
			Spent catalyst	6.03E−06	kg

4.2.2. Contribution of processes

In order to identify the processes with the highest impact on the life-cycle performance of the system, the contributions to the individual impact categories are broken down in Fig. 6 and discussed in detail throughout this section.

The main contributors to CED_{nr} are electricity, the natural gas required by the biorefinery and the agricultural activity, while the percentages contributed by other processes are low. The pyrolysis plants are responsible for 70.8% of the overall electricity consumption of the processing plants (Table 4), which is closely linked to the drying of the biomass feedstock. In this sense, the use of a

Table 6
Characterization results for 1 MJ of synthetic biofuel.

Subsystem	ADP (g Sb eq)	AP (g SO_2 eq)	EP (g PO_4^{3-} eq)	GWP (g CO_2 eq)	CED_{nr} (MJ)
Agriculture	4.94E−02	4.60E−02	3.41E−02	−125.76	0.21
Biomass transport	5.35E−03	3.68E−03	9.57E−04	7.63E−01	1.24E−02
Pyrolysis plant	8.35E−02	0.13	2.16E−02	46.37	0.21
Bio-oil transport	2.17E−02	1.68E−02	3.86E−03	3.46	4.94E−02
Biorefinery plant	0.18	5.51E−02	1.23E−02	39.04	0.38
Total	0.34	0.25	7.29E−02	−36.13	0.87

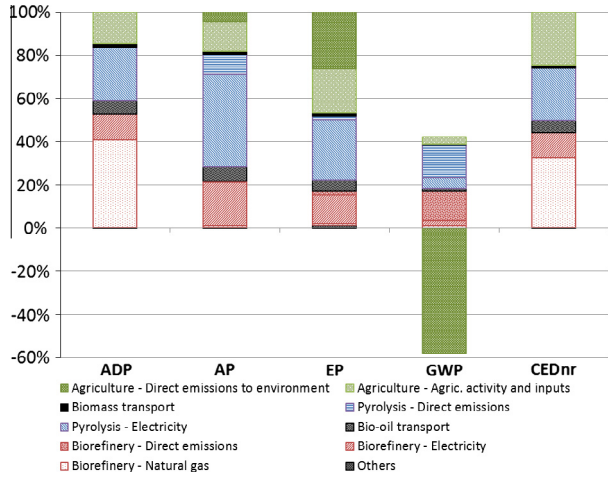

Fig. 6. Contribution of the processes to the potential environmental impacts.

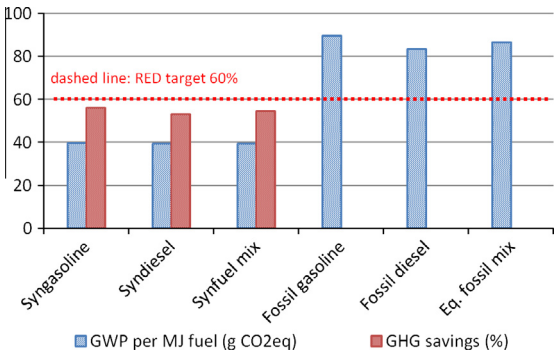

Fig. 8. Comparison of the well-to-wheels GWP impact (per MJ of fuel) of the synthetic biofuels with those of fossil gasoline and diesel.

drier feedstock would significantly improve the performance of the system. In the biorefinery, efforts for energy improvement should focus on reducing the natural gas demand in the steam reformer. Finally, in the agricultural phase reducing irrigation requirements would be an effective measure for improving the CED_{nr} result, as the electricity required for irrigation makes up over 80% of the contribution of this phase to CED_{nr}, followed by fertilizer production and tractor operation (these contributors do not appear explicitly in Fig. 6, but they are all contained in 'Agric. activity and inputs').

ADP shows an almost identical profile as CED_{nr}, indicating that fossil fuel depletion has the main impact on ADP, while mineral depletion has a significant influence only on the agricultural phase due to the fertilizers applied.

Electricity consumption is identified as the main source of AP, and environmental improvement regarding this impact category should hence focus on this aspect (by either reducing electricity consumption or using a greener electricity mix).

The agricultural phase contributes the main share to the total impact in the EP category, with direct impacts due to the leaching of eutrophying substances to the environment being slightly higher than indirect impacts related to agricultural activity such as plowing, irrigating, and fertilizing. Regarding indirect impacts ('Agric. activity and inputs' in Fig. 6), electricity consumption for irrigation makes up about half of the contribution, followed by fertilizer production and tractor operation, while the remaining agricultural activities do not contribute significantly. Another relevant contributor to EP is the electricity consumption of the plants, especially of the pyrolysis plants.

The GWP category is clearly dominated by the CO_2 uptake of the plantation in the cultivation phase. This is linked to the cradle-to-gate approach followed in this study, which does not include the combustion of the fuels. Apart from that, the main contribution to GWP comes from the direct emissions from the conversion plants. These stem principally from the combustion processes in the pyrolysis and steam reforming sections. Reducing the fuel consumption of the combustors should hence significantly enhance the performance of the system in this regard. Significant potential exists especially in the pyrolysis plants, where the main heat

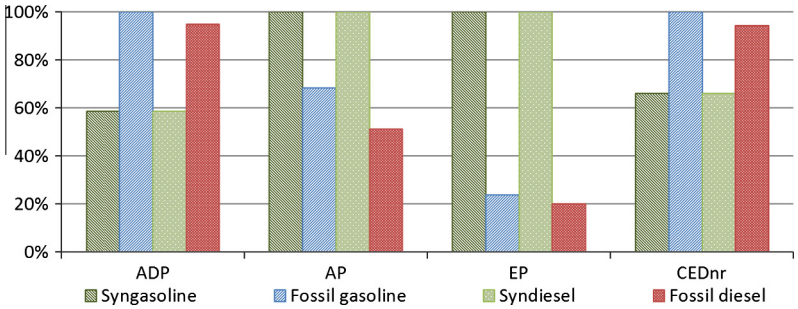

Fig. 7. Comparison (energy basis) of the potential environmental impacts of the synthetic biofuels with those of fossil gasoline and diesel.

Table A1
Main inventory data of the agricultural phase (poplar short-rotation plantation).

Inputs			Outputs		
Item	Amount	Unit	Item	Amount	Unit
Resources			*Products*		
Land occupation	0.37	m^2a	Hybrid poplar, SRC, u = 50	1.00	kg
Carbon fixation, from air, as CO_2	1.01	kg			
Irrigation water	0.15	m^3	*Emissions to air*		
			Ammonia	4.86E−05	kg
Transport and agricultural activity			Dinitrogen monoxide	4.78E−05	kg
Tractor and trailer (wood chips)	4.70E−02	t km	Nitrogen oxides, as NO_2	1.00E−05	kg
Agricultural activity	5.43E−05	ha			
			Emissions to water		
Chemicals and fertilizers			Nitrate	9.72E−04	kg
Ammonium nitrate, as N	2.00E−03	kg	Phosphorus	6.48E−06	kg
Triple superphosphate, as P_2O_5	3.33E−04	kg	Phosphate	7.95E−06	kg
Potassium chloride, as K_2O	1.20E−03	kg			
Pesticides	1.36E−05	l			

demand comes from the biomass dryer and the use of wood with lower moisture content could significantly improve the GWP performance.

4.2.3. Comparison with fossil fuels

Fig. 7 compares the life-cycle profile of the pyrolysis fuels with that of the equivalent fossil fuels taken from the ecoinvent database [47]. The GWP category is excluded in this figure, as it is discussed under a different perspective later in this section.

It can be observed that the impact of the pyrolysis fuels is lower than that of the fossil fuels for ADP and CED_{nr}, but higher for AP and EP. In particular, they show a significantly higher impact for EP, with the agricultural phase contributing an important share.

When evaluating the GWP category, it is recommendable to change the focus from a cradle-to-gate to a well-to-wheels perspective, including the fuel combustion in vehicle engines. Since the synthetic fuels have properties similar to those of conventional fossil fuels and show similar emission profiles, the same GHG emissions factors can be applied. Calculating with average emissions due to combustion according to EMEP/EEA [82], final GHG emission potentials of 39.41 g CO_2 eq MJ^{-1} and 39.13 g CO_2 - eq MJ^{-1} are obtained for the synthetic gasoline and the synthetic diesel, respectively (Fig. 8). The comparison with conventional gasoline and diesel leads to GHG emission savings of 55.9% (gasoline) and 53.0% (diesel) according to the RED methodology. For the fuel production mix (0.51 MJ gasoline and 0.49 MJ diesel), the equivalent savings would be 54.5%, a value close to the RED target of 60% [1]. Compared to the GHG savings of 60–88% reported by other works [18,19,21], this is a lower value, but these works mainly use agricultural residues as feedstock or use very simplified inventories for the agricultural phase, which is an important factor for the performance of the system. For hybrid poplar with comparable moisture content as feedstock and natural gas as hydrogen source for the hydrotreating process, Hsu et al. [20] report GHG savings of 53%, a value similar to that calculated in this study.

5. Conclusions

The simulation of the biofuel process chain based on fast pyrolysis of poplar biomass and subsequent hydroupgrading of the obtained bio-oil shows a good correlation with experimental works published in this field. The high amount of model compounds used for the bio-oil and the synthetic biofuels result in detailed inventories for the life cycle assessment of the system. Emissions of elements such as sulfur or chlorine are modeled explicitly, allowing the calculation of the corresponding environmental impacts. The biofuel system assessed shows GHG savings of 54.5% for the produced fuel mix. Abiotic depletion potential and non-renewable energy demand are significantly lower than those of fossil gasoline and diesel. However, higher impacts are obtained in other categories such as acidification and eutrophication, a pattern typical for biofuels.

Electricity consumption is identified as one of the keys for reducing the life-cycle impact in all of the assessed categories. Especially the biomass dryer in the pyrolysis plant shows high impacts due to the electricity consumption of the air compressors. Thus, an efficient measure for improving the plant performance would be the use of wood with lower moisture content or the installation of a passive pre-drying during biomass storage. Regarding GHG emissions, the direct emissions from the pyrolysis plants and the biorefinery are the main contributors, mainly due to the combustion processes for generating process heat. The drying stage is crucial also for this category, since the main share of the thermal energy generated by the combustor is demanded by the biomass dryer. The natural gas required by the hydroupgrading plays an important role in the abiotic depletion and non-renewable energy demand categories, but contributes little to the other assessed categories. Significant improvement potential is also identified in the agricultural phase, even though low-input short-rotation crops are used as feedstock. Reducing the irrigation water demand turns out to be the key for further reducing the environmental impacts caused in this stage. Overall, the system shows high GHG savings along with a still significant improvement potential and can be considered an interesting option for producing fuels from lignocellulosic biomass.

Acknowledgements

This research has been partly supported by the Regional Government of Madrid (S2009/ENE-1743) and the Spanish Ministry of Economy and Competitiveness (ENE2011-29643-C02-01 and IPT-2012-0219-120000).

Appendix A

Table A1 presents the main inventory data of the agricultural phase (hybrid poplar).

Tables A2–A6 present the stream tables from the Aspen Plus® simulation carried out in this article. The stream names correspond to the ones used in the flowsheets (Figs. 2–5). Streams with mass flows below 0.001 kg s^{-1} are omitted.

Table A2
Stream table of the pyrolysis section: conventional and mixed streams.

Stream	PYR-OUT	QENCHLIQ	FLUEGAS	PRODGAS	BIOOIL	COMBAIR	DRYINGAS	EXHSTGAS	QCHWATER	PYCLWTRIN	PYCWTOUT
Temperature K	793.0	304.1	304.0	304.0	289.3	298.5	650.0	375.4	298.5	298.5	315.6
Pressure N m^{-2}	2.38E+05	2.38E+05	1.06E+05	1.06E+05	1.06E+05	1.01E+05	1.26E+05	1.01E+05	1.01E+05	1.01E+05	1.01E+05
Mass flow kg s^{-1}	16.543	152.081	8.479	1.151	5.556	64.263	66.121	73.057	1.298	216	216
Conventional											
Mass flow kg s^{-1}	15.178	151.86	8.479	1.151	5.548	64.263	66.121	73.056	1.298	216	216
Water	1.237	29.203	0.15	0.02	1.067	0	0.755	7.69	1.298	216	216
N_2	0	0	0	0	0	50.768	50.783	50.783	0	0	0
OXYGEN	0	0	0	0	0	13.495	10.648	10.648	0	0	0
CO_2	2.899	0.431	2.539	0.345	0.016	0	3.93	3.93	0	0	0
CO	3.112	0.035	2.739	0.372	0.001	0	0	0	0	0	0
CH_4	0.432	0.012	0.38	0.052	0	0	0	0	0	0	0
ETHANE	0.046	0.011	0.04	0.005	0	0	0	0	0	0	0
ETHENE	0.218	0.031	0.191	0.026	0.001	0	0	0	0	0	0
PROPENE	0.604	0.447	0.517	0.07	0.016	0	0	0	0	0	0
H_2	0.119	0	0.105	0.014	0	0	0	0	0	0	0
H_2S	0.005	0.002	0.005	0.001	0	0	0	0	0	0	0
SO_2	0	0	0	0	0	0	0.002	0.002	0	0	0
NO_2	0	0	0	0	0	0	0	0	0	0	0
NO	0	0	0	0	0	0	0.002	0.002	0	0	0
AMMONIA	0.015	0.058	0.012	0.002	0.002	0	0	0	0	0	0
HCN	0.087	0.588	0.058	0.008	0.021	0	0	0	0	0	0
HCl	0.002	0	0.002	0	0	0	0.001	0.001	0	0	0
ACETICAC	0.214	5.462	0.012	0.002	0.2	0	0	0	0	0	0
FORMICAC	0.027	0.62	0.004	0.001	0.023	0	0	0	0	0	0
PROPNCAC	0.045	1.219	0.001	0	0.045	0	0	0	0	0	0
PHENOL	0.014	0.388	0	0	0.014	0	0	0	0	0	0
ACETOL	0.054	1.46	0.001	0	0.053	0	0	0	0	0	0
ACETALDY	1.06	3.025	0.836	0.114	0.111	0	0	0	0	0	0
GLYCOALD	0.644	17.552	0.003	0	0.641	0	0	0	0	0	0
FORMALDY	0.542	2.082	0.41	0.056	0.076	0	0	0	0	0	0
GLYOXAL	0.287	3.615	0.137	0.019	0.132	0	0	0	0	0	0
KETENE	0.026	0.017	0.022	0.003	0.001	0	0	0	0	0	0
ACETONE	0.425	3.446	0.263	0.036	0.126	0	0	0	0	0	0
NAPHTLEN	0.044	1.199	0	0	0.044	0	0	0	0	0	0
XYLOSE	0.002	0.049	0	0	0.002	0	0	0	0	0	0
LEVOGLUC	1.242	33.995	0	0	1.242	0	0	0	0	0	0
FURFURAL	0	0.004	0	0	0	0	0	0	0	0	0
HDRMTFUR	0.327	8.955	0	0	0.327	0	0	0	0	0	0
METHANOL	0.094	1.991	0.019	0.003	0.073	0	0	0	0	0	0
ETHANOL	0.075	1.368	0.022	0.003	0.05	0	0	0	0	0	0
ETYLDIOL	0.071	1.946	0	0	0.071	0	0	0	0	0	0
SINPYALC	0	0.007	0	0	0	0	0	0	0	0	0
CMRYLALC	0.709	19.157	0.008	0.001	0.7	0	0	0	0	0	0
MGUAIACOL	0.014	0.382	0	0	0.014	0	0	0	0	0	0
DEGR.LIG-1	0.028	0.765	0	0	0.028	0	0	0	0	0	0
DEGR.LIG-2	0.329	9	0	0	0.329	0	0	0	0	0	0
DEGR.LIG-3	0.008	0.23	0	0	0.008	0	0	0	0	0	0
PYRROLID	0	0.002	0	0	0	0	0	0	0	0	0
PYRROLE	0.118	3.106	0.004	0.001	0.113	0	0	0	0	0	0
Solids											
Mass flow kg s^{-1}	1.365	0.222	0	0	0.008	0	0	0	0	0	0
WOOD	0	0	0	0	0	0	0	0	0	0	0
CHAR	1.365	0.222	0	0	0.008	0	0	0	0	0	0
ASH	0	0	0	0	0	0	0	0	0	0	0

Table A3
Stream table of the pyrolysis section: pure solid streams.

Stream	BIOM-WET	BIOMFEED	CHARCOMB	CHARPROD	ASHOUT
Temperature K	298.50	325	793	793	1000
Mass flow kg s^{-1}	15	8.065	0.83	0.527	0.123
Moisture	50.00	7.00	0.00	0.00	0.00
Atomic composition					
ASH	2.70	2.70	14.83	14.83	100.00
CARBON	50.20	50.20	68.65	68.65	0.00
HYDROGEN	6.06	6.06	2.39	2.39	0.00
NITROGEN	0.80	0.80	1.31	1.31	0.00
CHLORINE	0.01	0.01	0.03	0.03	0.00
SULFUR	0.02	0.02	0.06	0.06	0.00
OXYGEN	40.22	40.22	12.72	12.72	0.00

Table A4
Stream table of the hydrotreating section of the biorefinery.

Stream	BIOOIL	HTH2FEED	HT1FEED	HT1OUT	HT2OUT	HTORGANC	HTAQUOUS	STEAMCLD	STEAMHOT	HTCLWTIN	HTCLWOUT
Temperature K	289.3	345.0	525.0	645.1	645.1	295.9	295.9	475.0	580.3	298.5	314.4
Pressure N m^{-2}	1.06E+05	4.50E+06	1.70E+07	1.39E+07	1.39E+07	3.50E+06	3.50E+06	2.00E+06	2.00E+06	1.01E+05	1.06E+05
Mass flow kg s^{-1}	5.548	0.5	6.048	6.048	6.048	3.461	2.587	2.823	2.823	49.274	49.274
WATER	1.067	0	1.067	2.526	2.526	0.003	2.523	2.823	2.823	49.274	49.274
CO_2	0.016	0	0.016	0.647	0.647	0.647	0	0	0	0	0
CO	0.001	0	0.001	0.043	0.043	0.043	0	0	0	0	0
CH_4	0	0	0	0.139	0.139	0.139	0	0	0	0	0
ETHANE	0	0	0	0.023	0.023	0.023	0	0	0	0	0
ETHENE	0.001	0	0.001	0.012	0.012	0.012	0	0	0	0	0
PROPANE	0	0	0	0.023	0.023	0.023	0	0	0	0	0
PROPENE	0.016	0	0.016	0.012	0.012	0.012	0	0	0	0	0
BUTANE	0	0	0	0.033	0.033	0.033	0	0	0	0	0
H_2	0	0.5	0.5	0.294	0.294	0.294	0	0	0	0	0
AMMONIA	0.002	0	0.002	0.044	0.044	0.002	0.043	0	0	0	0
HCN	0.021	0	0.021	0	0	0	0	0	0	0	0
ACETICAC	0.2	0	0.2	0	0	0	0	0	0	0	0
FORMICAC	0.023	0	0.023	0	0	0	0	0	0	0	0
PROPNCAC	0.045	0	0.045	0	0	0	0	0	0	0	0
PHENOL	0.014	0	0.014	0.008	0.008	0.001	0.008	0	0	0	0
CRESOL	0	0	0	0.003	0.003	0.001	0.002	0	0	0	0
XYELNOL	0	0	0	0.003	0.003	0.001	0.001	0	0	0	0
ETYLPHEN	0	0	0	0.003	0.003	0.003	0	0	0	0	0
PRPNYPHN	0	0	0	0.008	0.008	0.008	0	0	0	0	0
BENZENE	0	0	0	0.056	0.056	0.056	0	0	0	0	0
TOLUENE	0	0	0	0.012	0.012	0.012	0	0	0	0	0
M-XYLENE	0	0	0	0.012	0.012	0.012	0	0	0	0	0
ETYLBZNE	0	0	0	0.012	0.012	0.012	0	0	0	0	0
PROPBENZ	0	0	0	0.046	0.046	0.046	0	0	0	0	0
ACETOL	0.053	0	0.053	0	0	0	0	0	0	0	0
ACETALDY	0.111	0	0.111	0	0	0	0	0	0	0	0
GLYCOALD	0.641	0	0.641	0	0	0	0	0	0	0	0
FORMALDY	0.076	0	0.076	0	0	0	0	0	0	0	0
GLYOXAL	0.132	0	0.132	0	0	0	0	0	0	0	0
KETENE	0.001	0	0.001	0	0	0	0	0	0	0	0
ACETONE	0.126	0	0.126	0	0	0	0	0	0	0	0
PENTANE	0	0	0	0.042	0.042	0.042	0	0	0	0	0
HEXANE	0	0	0	0.064	0.064	0.064	0	0	0	0	0
HEPTAN	0	0	0	0.058	0.058	0.058	0	0	0	0	0
OCTANE	0	0	0	0.06	0.06	0.06	0	0	0	0	0
NONANE	0	0	0	0.07	0.07	0.07	0	0	0	0	0
DECANE	0	0	0	0.06	0.06	0.06	0	0	0	0	0
UNDECAN	0	0	0	0.06	0.06	0.06	0	0	0	0	0
DODECAN	0	0	0	0.07	0.07	0.07	0	0	0	0	0
TRIDECAN	0	0	0	0.065	0.065	0.065	0	0	0	0	0
TETDECAN	0	0	0	0.065	0.065	0.065	0	0	0	0	0
PENTDECA	0	0	0	0.07	0.07	0.07	0	0	0	0	0
OCTDECAN	0	0	0	0.07	0.07	0.07	0	0	0	0	0
CYCPNTAN	0	0	0	0.065	0.065	0.065	0	0	0	0	0
CYCHEXEN	0	0	0	0.112	0.112	0.112	0	0	0	0	0
CYCHEXAN	0	0	0	0.152	0.152	0.152	0	0	0	0	0
MTHCYCPT	0	0	0	0.109	0.109	0.109	0	0	0	0	0
MTCYCHXA	0	0	0	0.109	0.109	0.109	0	0	0	0	0
PRCYCHXA	0	0	0	0.152	0.152	0.152	0	0	0	0	0
BICYCHEX	0	0	0	0.088	0.088	0.088	0	0	0	0	0
BICYPRHX	0	0	0	0.088	0.088	0.088	0	0	0	0	0
NAPHTLEN	0.044	0	0.044	0.024	0.024	0.024	0	0	0	0	0
CHRYSENE	0	0	0	0.321	0.321	0.321	0	0	0	0	0
XYLOSE	0.002	0	0.002	0	0	0	0	0	0	0	0
LEVOGLUC	1.242	0	1.242	0	0	0	0	0	0	0	0
FURFURAL	0	0	0	0.001	0.001	0	0	0	0	0	0
FURFYALC	0	0	0	0.001	0.001	0	0.001	0	0	0	0
HDRMTFUR	0.327	0	0.327	0.004	0.004	0	0.004	0	0	0	0
FURAN	0	0	0	0.029	0.029	0.029	0	0	0	0	0
DIMTYFUR	0	0	0	0.04	0.04	0.04	0	0	0	0	0
METHANOL	0.073	0	0.073	0.005	0.005	0	0.005	0	0	0	0
ETHANOL	0.05	0	0.05	0.004	0.004	0.003	0.001	0	0	0	0
PROPANOL	0	0	0	0.004	0.004	0.004	0	0	0	0	0
BUTANOL	0	0	0	0.004	0.004	0.004	0	0	0	0	0
HEXANOL	0	0	0	0.004	0.004	0.004	0	0	0	0	0
PENTANOL	0	0	0	0.004	0.004	0.004	0	0	0	0	0
ETYLDIOL	0.071	0	0.071	0	0	0	0	0	0	0	0
CYCHXNOL	0	0	0	0.009	0.009	0.009	0	0	0	0	0
PRCYHXOL	0	0	0	0.009	0.009	0.009	0	0	0	0	0
CMRYLALC	0.7	0	0.7	0	0	0	0	0	0	0	0

Table A4 (*continued*)

Stream	BIOOIL	HTH2FEED	HT1FEED	HT1OUT	HT2OUT	HTORGANC	HTAQUOUS	STEAMCLD	STEAMHOT	HTCLWTIN	HTCLWOUT
MGUAIACOL	0.014	0	0.014	0	0	0	0	0	0	0	0
DEGR.LIG-1	0.028	0	0.028	0	0	0	0	0	0	0	0
DEGR.LIG-2	0.329	0	0.329	0	0	0	0	0	0	0	0
DEGR.LIG-3	0.008	0	0.008	0	0	0	0	0	0	0	0
PYRROLE	0.113	0	0.113	0	0	0	0	0	0	0	0

Table A5
Stream table of the distillation and hydrocracking section of the biorefinery.

Stream	HTORGANC	FLSHGAS	DISTFEED	DISTGAS	GASLNOUT	D1BOTTOM	DIESLOUT	D2BOTTOM	HCRACKIN	HCH2FEED	HCRCKOUT	HCCLWTIN	HCCLWOUT
Temperature K	295.9	295.2	430.0	305.0	305.0	532.0	329.3	551.1	915.0	345.0	948.1	298.5	314.9
Pressure N m^{-2}	3.50E+06	2.00E+06	3.90E+05	2.30E+05	2.30E+05	2.83E+05	1.00E+03	2.00E+03	8.98E+06	4.50E+06	8.89E+06	1.01E+05	1.21E+05
Mass flow kg s^{-1}	3.461	1.331	2.402	0.027	1.115	1.259	1.066	0.193	0.272	0.078	0.272	35.394	35.394
Conventional													
Mass flow kg s^{-1}	3.461	1.331	2.402	0.027	1.115	1.259	1.066	0.193	0.272	0.078	0.272	35.394	35.394
WATER	0.003	0.001	0.002	0	0.002	0	0	0	0	0	0	35.394	35.394
CO_2	0.647	0.621	0.026	0.016	0.01	0	0	0	0	0	0	0	0
CO	0.043	0.043	0	0	0	0	0	0	0	0	0	0	0
CH_4	0.139	0.141	0.001	0.001	0	0	0	0	0	0	0.003	0	0
ETHANE	0.023	0.024	0.001	0.001	0.001	0	0	0	0	0	0.002	0	0
ETHENE	0.012	0.012	0	0	0	0	0	0	0	0	0	0	0
PROPANE	0.023	0.022	0.005	0.001	0.004	0	0	0	0	0	0.004	0	0
PROPENE	0.012	0.01	0.002	0	0.001	0	0	0	0	0	0	0	0
BUTANE	0.033	0.022	0.016	0.001	0.015	0	0	0	0	0	0.005	0	0
H_2	0.294	0.352	0	0	0	0	0	0	0.078	0.078	0.059	0	0
AMMONIA	0.002	0.001	0	0	0	0	0	0	0	0	0	0	0
PHENOL	0.001	0	0.001	0	0	0	0	0	0	0	0	0	0
CRESOL	0.001	0	0.001	0	0	0.001	0.001	0	0	0	0	0	0
XYELNOL	0.001	0	0.001	0	0	0.001	0.001	0	0	0	0	0	0
ETYLPHEN	0.003	0	0.003	0	0	0.003	0.003	0	0	0	0	0	0
PRPNYPHN	0.008	0	0.008	0	0	0.008	0.008	0	0	0	0	0	0
BENZENE	0.056	0.005	0.058	0	0.058	0	0	0	0	0	0.007	0	0
TOLUENE	0.012	0	0.019	0	0.019	0	0	0	0	0	0.008	0	0
M-XYLENE	0.012	0	0.02	0	0.018	0.002	0.002	0	0	0	0.009	0	0
ETYLBZNE	0.012	0	0.011	0	0.01	0.001	0.001	0	0	0	0	0	0
PROPBENZ	0.046	0	0.055	0	0.031	0.025	0.025	0	0	0	0.01	0	0
PENTANE	0.042	0.013	0.035	0.001	0.034	0	0	0	0	0	0.006	0	0
HEXANE	0.064	0.007	0.059	0	0.058	0	0	0	0	0	0.001	0	0
HEPTAN	0.058	0.002	0.056	0	0.055	0	0	0	0	0	0	0	0
OCTANE	0.06	0.001	0.069	0	0.067	0.001	0.001	0	0	0	0.01	0	0
NONANE	0.07	0	0.077	0	0.052	0.024	0.024	0	0	0	0.007	0	0
DECANE	0.06	0	0.066	0	0.017	0.049	0.049	0	0	0	0.006	0	0
UNDECAN	0.06	0	0.077	0	0.001	0.077	0.077	0	0	0	0.017	0	0
DODECAN	0.07	0	0.081	0	0	0.081	0.081	0	0	0	0.011	0	0
TRIDECAN	0.065	0	0.075	0	0	0.075	0.075	0	0	0	0.01	0	0
TETDECAN	0.065	0	0.078	0	0	0.078	0.078	0	0	0	0.013	0	0
PENTDECA	0.07	0	0.088	0	0	0.088	0.088	0	0	0	0.018	0	0
OCTDECAN	0.07	0	0.085	0	0	0.085	0.085	0	0	0	0.015	0	0
CYCPNTAN	0.065	0.012	0.057	0.001	0.056	0	0	0	0	0	0.004	0	0
CYCHEXEN	0.112	0.007	0.105	0	0.104	0	0	0	0	0	0	0	0
CYCHEXAN	0.152	0.011	0.149	0.001	0.148	0	0	0	0	0	0.007	0	0
MTHCYCPT	0.109	0.009	0.099	0.001	0.099	0	0	0	0	0	0	0	0
MTCYCHXA	0.109	0.004	0.113	0	0.113	0	0	0	0	0	0.008	0	0
PRCYCHXA	0.152	0.001	0.159	0	0.059	0.1	0.1	0	0	0	0.007	0	0
BICYCHEX	0.088	0	0.102	0	0	0.102	0.102	0	0	0	0.014	0	0
BICYPRHX	0.088	0	0.088	0	0	0.088	0.088	0	0	0	0	0	0
NAPHTLEN	0.024	0	0.035	0	0	0.035	0.035	0	0	0	0.011	0	0
CHRYSENE	0.321	0	0.321	0	0	0.321	0.128	0.193	0.193	0	0	0	0
FURAN	0.029	0.009	0.02	0.001	0.02	0	0	0	0	0	0	0	0
DIMTYFUR	0.04	0.001	0.039	0	0.039	0	0	0	0	0	0	0	0
ETHANOL	0.003	0	0.003	0	0.003	0	0	0	0	0	0	0	0
PROPANOL	0.004	0	0.004	0	0.004	0	0	0	0	0	0	0	0
BUTANOL	0.004	0	0.004	0	0.004	0	0	0	0	0	0	0	0
HEXANOL	0.004	0	0.004	0	0.002	0.001	0.001	0	0	0	0	0	0
PENTANOL	0.004	0	0.004	0	0.004	0	0	0	0	0	0	0	0
CYCHXNOL	0.009	0	0.009	0	0.005	0.003	0.003	0	0	0	0	0	0
PRCYHXOL	0.009	0	0.009	0	0	0.008	0.008	0	0	0	0	0	0

Table A6
Stream table of the steam reforming section of the biorefinery.

Stream	FLSHGAS	HTAQUOUS	SRAQUIN	SRGASRCT	SRCH4EXT	SRRCTIN	SRRCTOUT	SRWGSOUT	SROFFGAS1	SRH2THDO	SRH2THCR	DISTGAS	SRCMBAIR	SRCMBIN	SRCMBEXG	SRLIQOUT	SRCLWTIN	SRCLWOUT
Temperature K	295.2	295.9	321.0	409.4	298.5	774.2	1223.2	623.1	350.0	350.0	350.0	305.0	295.0	1262.7	1363.7	350.2	298.5	314.3
Pressure N m^{-2}	2.00E+06	3.50E+06	3.50E+06	5.00E+06	5.00E+06	4.90E+06	4.85E+06	4.77E+06	2.70E+05	4.45E+06	4.45E+06	2.30E+05	1.01E+05	2.40E+05	1.90E+05	3.50E+06	1.01E+05	1.06E+05
Mass flow kg s^{-1}	1.331	2.587	4.805	1.222	0.496	6.522	6.522	6.522	2.689	0.503	0.073	0.027	9.272	12.098	12.105	1.039	80	80
Conventional																		
Mass flow kg s^{-1}	1.331	2.587	4.805	1.222	0.496	6.522	6.522	6.522	2.689	0.503	0.073	0.027	9.272	12.098	12.105	1.039	80	80
WATER	0.001	2.523	4.739	0.001	0	4.739	3.866	3.317	0.063	0	0	0	0	0.063	1.257	1.038	80	80
N_2	0	0	0	0	0	0	0.036	0.036	0.036	0	0	0	7.325	7.361	7.36	0	0	0
OXYGEN	0	0	0	0	0	0	0	0	0	0	0	0	1.947	1.947	0.412	0	0	0
CO_2	0.621	0	0.001	0.57	0	0.572	0.849	2.19	2.188	0	0	0.016	0	2.255	3.074	0.001	0	0
CO	0.043	0	0	0.039	0	0.039	1.059	0.206	0.206	0	0	0	0	0.209	0	0	0	0
CH_4	0.141	0	0	0.129	0.496	0.625	0.132	0.132	0.132	0	0	0.001	0	0.145	0	0	0	0
ETHANE	0.024	0	0	0.022	0	0.022	0	0	0	0	0	0.001	0	0.003	0	0	0	0
ETHENE	0.012	0	0	0.011	0	0.011	0	0	0	0	0	0	0	0.001	0	0	0	0
PROPANE	0.022	0	0	0.021	0	0.021	0	0	0	0	0	0.001	0	0.003	0	0	0	0
PROPENE	0.01	0	0	0.01	0	0.01	0	0	0	0	0	0	0	0.001	0	0	0	0
BUTANE	0.022	0	0	0.02	0	0.02	0	0	0	0	0	0.001	0	0.003	0	0	0	0
H_2	0.352	0	0	0.323	0	0.323	0.579	0.64	0.064	0.503	0.073	0	0	0.093	0	0	0	0
NO	0	0	0	0	0	0	0	0	0	0	0	0	0	0	0.003	0	0	0
AMMONIA	0.001	0.043	0.043	0.001	0	0.045	0.001	0.001	0	0	0	0	0	0.001	0	0	0	0
PHENOL	0	0.008	0.008	0	0	0.008	0	0	0	0	0	0	0	0	0	0	0	0
CRESOL	0	0.002	0.002	0	0	0.002	0	0	0	0	0	0	0	0	0	0	0	0
XYELNOL	0	0.001	0.001	0	0	0.001	0	0	0	0	0	0	0	0	0	0	0	0
BENZENE	0.005	0	0	0.004	0	0.004	0	0	0	0	0	0	0	0.001	0	0	0	0
PENTANE	0.013	0	0	0.012	0	0.012	0	0	0	0	0	0.001	0	0.002	0	0	0	0
HEXANE	0.007	0	0	0.006	0	0.006	0	0	0	0	0	0	0	0.001	0	0	0	0
HEPTAN	0.002	0	0	0.002	0	0.002	0	0	0	0	0	0	0	0	0	0	0	0
OCTANE	0.001	0	0	0.001	0	0.001	0	0	0	0	0	0	0	0	0	0	0	0
CYCPNTAN	0.012	0	0	0.011	0	0.011	0	0	0	0	0	0.001	0	0.002	0	0	0	0
CYCHEXEN	0.007	0	0	0.006	0	0.006	0	0	0	0	0	0	0	0.001	0	0	0	0
CYCHEXAN	0.011	0	0	0.01	0	0.01	0	0	0	0	0	0.001	0	0.002	0	0	0	0
MTHCYCPT	0.009	0	0	0.009	0	0.009	0	0	0	0	0	0.001	0	0.001	0	0	0	0
MTCYCHXA	0.004	0	0	0.003	0	0.003	0	0	0	0	0	0	0	0.001	0	0	0	0
PRCYCHXA	0.001	0	0	0.001	0	0.001	0	0	0	0	0	0	0	0	0	0	0	0
FURFYALC	0	0.001	0.001	0	0	0.001	0	0	0	0	0	0	0	0	0	0	0	0
HDRMTFUR	0	0.004	0.004	0	0	0.004	0	0	0	0	0	0	0	0	0	0	0	0
FURAN	0.009	0	0	0.008	0	0.008	0	0	0	0	0	0.001	0	0.001	0	0	0	0
DIMTYFUR	0.001	0	0	0.001	0	0.001	0	0	0	0	0	0	0	0	0	0	0	0
METHANOL	0	0.005	0.005	0	0	0.005	0	0	0	0	0	0	0	0	0	0	0	0
ETHANOL	0	0.001	0.001	0	0	0.001	0	0	0	0	0	0	0	0	0	0	0	0

References

[1] EC. Directive 2009-28-EC on the promotion of the use of energy from renewable sources. Brussels, (Belgium): European Parliament and the Council; 2009.
[2] Von Blottnitz H, Curran MA. A review of assessments conducted on bio-ethanol as a transportation fuel from a net energy, greenhouse gas, and environmental life cycle perspective. J Clean Prod 2007;15:607–19.
[3] Holzschuh A, Dormann CF, Tscharntke T, Steffan-Dewenter I. Expansion of mass-flowering crops leads to transient pollinator dilution and reduced wild plant pollination. Proc Biol Sci 2011;278:3444–51.
[4] Russi D. An integrated assessment of a large-scale biodiesel production in Italy: killing several birds with one stone? Energ Policy 2008;36:1169–80.
[5] Zah R, Böni H, Gauch M, Hischier R, Lehmann M, Wäger P. Life cycle assessment of energy products: environmental assessment of biofuels – executive summary. Bern, Switzerland: EMPA – Materials Science & Technology, Federal Office for Energy (BFE); 2006.
[6] Fargione JE, Plevin RJ, Hill JD. The ecological impact of biofuels. Ann Rev Ecol, Evol, Syst 2010;41:351–77.
[7] EC. Proposal for a directive of the european parliament and of the council amending directive 98/70/EC relating to the quality of petrol and diesel fuels and amending Directive 2009/28/EC on the promotion of the use of energy from renewable sources. Brussels, Belgium: European Commission; 2012.
[8] EEA. EU bioenergy potential from a resource efficiency perspective – EEA Report No 6/2013. Copenhagen, Denmark: 2013.
[9] Peters JF, Petrakopoulou F, Dufour J. Exergetic analysis of a fast pyrolysis process for bio-oil production. Fuel Process Technol 2014;119:245–55.
[10] Bridgwater AV. Fast pyrolysis processes for biomass. Renew Sust Energ Rev 2000;4:1–73.
[11] Bridgwater AV. Biomass fast pyrolysis. Therm Sci 2004;8:21–49.
[12] Chiaramonti D, Oasmaa A, Solantausta Y. Power generation using fast pyrolysis liquids from biomass. Renew Sust Energ Rev 2007;11:1056–86.
[13] Czernik S, Bridgwater AV. Overview of applications of biomass fast pyrolysis oil. Energ Fuel 2004;18:590–8.
[14] Pollex A, Ortwein A, Kaltschmitt M. Thermo-chemical conversion of solid biofuels. Biom Conv Bioref 2011;2:21–39.
[15] Bridgwater AV. Upgrading biomass fast pyrolysis liquids. Environ Prog Sustain Energ 2012;31:261–8.
[16] Elliott DC. Advancement of bio-oil utilization for refinery feedstock. The Washington Bioenergy Research Symposium. Washington (United States): PNNL; 2010.
[17] Elliott DC. Historical developments in hydroprocessing bio-oils. Energ Fuel 2007;21:1792–815.
[18] Iribarren D, Peters JF, Dufour J. Life cycle assessment of transportation fuels from biomass pyrolysis. Fuel 2012;97:812–21.
[19] Iribarren D, Peters JF, Petrakopoulou F, Dufour J. Well-to-wheels comparison of the environmental profile of pyrolysis-based biofuels. In: 20th European biomass conference and exhibition, Milan, Italy; 2012.
[20] Hsu DD. Life cycle assessment of gasoline and diesel produced via fast pyrolysis and hydroprocessing. Biomass Bioenerg 2012;45:41–7.
[21] Han J, Elgowainy A, Dunn JB, Wang MQ. Life cycle analysis of fuel production from fast pyrolysis of biomass. Bioresour Technol 2013;133C:421–8.
[22] Udo de Haes HA, Heijungs R. Life-cycle assessment for energy analysis and management. Appl Energ 2007;84:817–27.
[23] ISO. ISO 14040 – Environmental management – life cycle assessment – principles and framework; 2006.
[24] ISO. ISO 14044 – environmental management – life cycle assessment – requirements and guideline; 2006.
[25] Cherubini F, Strømman AH. Life cycle assessment of bioenergy systems: state of the art and future challenges. Bioresour Technol 2011;102:437–51.
[26] Malça J, Freire F. Life-cycle studies of biodiesel in Europe: a review addressing the variability of results and modeling issues. Renew Sust Energ Rev 2011;15:338–51.
[27] Muench S, Guenther E. A systematic review of bioenergy life cycle assessments. Appl Energ 2013;112:257–73.
[28] Han J, Elgowainy A, Palou-Rivera I, Dunn JB, Wang MQ. Well-to-wheels analysis of fast pyrolysis pathways with GREET. Chicago (United States): Argonne National Laboratories; 2011.
[29] Steele P, Penmetsa K, Puettmann M, Cooper J. Producing liquid fuels from pyrolysis of woody biomass. Starkville (United States): Mississippi State University; 2008.
[30] Kauffman N, Hayes D, Brown R. A life cycle assessment of advanced biofuel production from a hectare of corn. Fuel 2011;90:3306–14.
[31] Dang Q, Yu C, Luo Z. Environmental life cycle assessment of bio-fuel production via fast pyrolysis of corn stover and hydroprocessing. Fuel 2014;131:36–42.
[32] Meier D, van de Beld B, Bridgwater AV, Elliott DC, Oasmaa A, Preto F. State-of-the-art of fast pyrolysis in IEA bioenergy member countries. Renew Sust Energ Rev 2013;20:619–41.
[33] Ringer M, Putsche V, Scahill J. Large-scale pyrolysis oil production: a technology assessment and economic analysis. (Golden) United States: National Renewable Energy Laboratory; 2006.
[34] Jones SB, Valkenburg C, Walton CW, Elliott DC, Holladay JE, Stevens DJ, et al. Production of gasoline and diesel from biomass via fast pyrolysis, hydrotreating and hydrocracking: a design case. (Washington) United States: Pacific Northwest National Laboratory; 2009.
[35] Wright MM, Satrio JA, Brown RC, Daugaard DE, Hsu DD. Techno-economic analysis of biomass fast pyrolysis to transportation fuels. (Golden) United States: National Renewable Energy Laboratory; 2010.
[36] Brown TR, Thilakaratne R, Brown RC, Hu G. Techno-economic analysis of biomass to transportation fuels and electricity via fast pyrolysis and hydroprocessing. Fuel 2013;106:463–9.
[37] Aspen Technology. AspenPlus; 2012.
[38] Brander M, Tipper R, Hutchison C, Davis G. Consequential and attributional approaches to LCA: a guide to policy makers with specific reference to greenhouse gas LCA of biofuels. Technical Paper TP-090403-A. Ecometrica Publications; 2009.
[39] Zuwała J. Life cycle approach for energy and environmental analysis of biomass and coal co-firing in CHP plant with backpressure turbine. J Clean Prod 2012;35:164–75.
[40] Menten F, Chèze B, Patouillard L, Bouvart F. A review of LCA greenhouse gas emissions results for advanced biofuels: the use of meta-regression analysis. Renew Sust Energ Rev 2013;26:108–34.
[41] EEA. How much bioenergy can Europe produce without harming the environment? Copenhagen, Denmark: European Environment Agency; 2006.
[42] Leible L, Kälber S, Kappler G, Lange S, Nieke E, Proplesch P, et al. Kraftstoff, Strom und Wärme aus Stroh und Waldrestholz. Karlsruhe, Germany: KIT Institut für Technikfolgenabschätzung und Systemanalyse; 2007.
[43] Wright MM, Brown RC, Boateng AA. Distributed processing of biomass to bio-oil for subsequent production of Fischer-Tropsch liquids. Biofuel Bioprod Bior 2008;2:229–38.
[44] Wright MM, Daugaard DE, Satrio JA, Brown RC. Techno-economic analysis of biomass fast pyrolysis to transportation fuels. Fuel 2010;89:S2–S10.
[45] Peters JF, Iribarren D, Dufour J. Life cycle assessment of pyrolysis oil applications. Biom Conv Bioref 2014; [in press]. http://dx.doi.org/10.1007/s13399-014-0120-z.
[46] Althaus H-J, Doka G, Heck T, Hellweg S, Hischier R, Nemecek T, et al. Overview and methodology. In: Frischknecht R, Jungbluth N, editors. Sachbilanzen von Energiesystemen: Grundlagen für den ökologischen Vergleich von Energiesystemen und den Einbezug von Energiesystemen in Ökobilanzen für die Schweiz. ecoinvent report No. 1. Dübendorf, Switzerland: Swiss Centre for Life Cycle Inventories; 2007.
[47] Erdöl Jungbluth N. In: Dones R, editor. Sachbilanzen von Energiesystemen: Grundlagen für den ökologischen Vergleich von Energiesystemen und den Einbezug von Energiesystemen in Ökobilanzen für die Schweiz. ecoinvent report No. 4. Dübendorf, Switzerland: Swiss Centre for Life Cycle Inventories; 2007.
[48] Spielmann M, Bauer C, Dones R, Tuchschmid M. Transport services. Sachbilanzen von Energiesystemen: Grundlagen für den ökologischen Vergleich von Energiesystemen und den Einbezug von Energiesystemen in Ökobilanzen für die Schweiz. ecoinvent report No. 14, Dübendorf, Switzerland: Swiss Centre for Life Cycle Inventories; 2007.
[49] Althaus H-J, Chudacoff M, Hischier R, Jungbluth N, Osses M, Primas A. Life cycle inventories of chemicals. Sachbilanzen von Energiesystemen: Grundlagen für den ökologischen Vergleich von Energiesystemen und den Einbezug von Energiesystemen in Ökobilanzen für die Schweiz. ecoinvent report No. 8, Dübendorf, Switzerland: Swiss Centre for Life Cycle Inventories; 2007.
[50] Gasol CM, Martínez S, Rigola M, Rieradevall J, Anton A, Carrasco J, et al. Feasibility assessment of poplar bioenergy systems in the Southern Europe. Renew Sust Energ Rev 2009;13:801–12.
[51] Gasol CM, Gabarrell X, Anton A, Rigola M, Carrasco J, Ciria P, et al. LCA of poplar bioenergy system compared with Brassica carinata energy crop and natural gas in regional scenario. Biomass Bioenerg 2009;33:119–29.
[52] Phyllis2, database for biomass and waste [Internet]. Petten, The Netherlands: Energy research Centre of the Netherlands (ECN); 2012 [cited 2014 Sept 15]. Available from: https://www.ecn.nl/phyllis2/.
[53] Varela M. Large-scale economic integration of electricity from short-rotation woody crops. Sol Energy 2001;70:95–107.
[54] Deckmyn G, Laureysens I, Garcia J, Muys B, Ceulemans R. Poplar growth and yield in short rotation coppice: model simulations using the process model SECRETS. Biomass Bioenerg 2004;26:221–7.
[55] Nemecek T, Kägi T. Life cycle inventories of agricultural production systems. In: Dones R, editor. Sachbilanzen von Energiesystemen: Grundlagen für den ökologischen Vergleich von Energiesystemen und den Einbezug von Energiesystemen in Ökobilanzen für die Schweiz. ecoinvent report No. 1. Dübendorf, Switzerland: Swiss Centre for Life Cycle Inventories; 2007.
[56] Verchot L, Krug T, Lasco RD, Ogle S, Raison J, Li Y, et al. Grassland Chapter 6. In: Eggleston HS, Buendia L, Miwa K, Ngara T, Tanabe K, editors. IPCC guidelines for national greenhouse gas inventories. Agriculture. Forestry and Other Land Use, vol. 4. Japan: National Greenhouse Gas Inventories Programme, IGES; 2006.
[57] Bickel K, Richards G, Köhl M, Vianna Rodrigues RL, Stahl G. Consistent representation of lands Chapter 3. In: Eggleston HS, Buendia L, Miwa K, Ngara T, Tanabe K, editors. IPCC Guidelines for National Greenhouse Gas Inventories. Agriculture. Forestry and Other Land Use, vol. 4. Japan: National Greenhouse Gas Inventories Programme, IGES; 2006.
[58] Aalde H, Gonzalez P, Gytarsky M, Krug T, Kurz WA, Lasco RD, et al. Generic methodologies applicable to multiple land-use categories Chapter 2. In:

Eggleston HS, Buendia L, Miwa K, Ngara T, Tanabe K, editors. IPCC Guidelines for National Greenhouse Gas Inventories. Agriculture. Forestry and Other Land Use, vol. 4. Japan: National Greenhouse Gas Inventories Programme, IGES.
[59] Maciejewska A, Veringa H, Sanders J, Peteves SD. Co-firing of biomass with coal: Constraints and role of biomass pre-treatment. Luxembourg: 2006.
[60] Lynch S, Reno M. Sustainable biofuels from fast pyrolysis. In: Envergent Technologies, editor. APEC Workshop on implications of Bio-refineries for Energy and Trade in the APEC Region, Taipei, Chinese Taipei; 2009.
[61] Mani S. A systems analysis of biomass densification processes. PhD Thesis. Vancouver, Canada: University of British Columbia, Dept. of Chemical & Biological Engineering; 2005.
[62] Peters JF, Iribarren D, Dufour J. Predictive pyrolysis process modelling in Aspen Plus. In: 21st European Biomass Conference and Exhibition, Copenhagen, Denmark; 2013.
[63] Bridgwater AV. Fast pyrolysis requirements for fuels and chemicals. In: From Biomass to Bioenergy via Thermochemical Processes. Stellenbosch, South Africa: Aston University Bioenergy Research Group; 2012.
[64] Lievens C, Yperman J, Vangronsveld J, Carleer R. Study of the potential valorisation of heavy metal contaminated biomass via phytoremediation by fast pyrolysis: Part I. Influence of temperature, biomass species and solid heat carrier on the behaviour of heavy metals. Fuel 2008;87:1894–905.
[65] Lievens C, Carleer R, Cornelissen T, Yperman J. Fast pyrolysis of heavy metal contaminated willow: influence of the plant part. Fuel 2009;88:1417–25.
[66] Agblevor FA, Besler S. Inorganic compounds in biomass feedstocks. 1. Effect on the quality of fast pyrolysis oils. Energ Fuel 1996;10:293–8.
[67] Venderbosch RH, Ardiyanti AR, Wildschut J, Oasmaa A, Heeres HJ. Stabilization of biomass-derived pyrolysis oils. J Chem Technol Biot 2010;85:674–86.
[68] De Miguel Mercader F, Groeneveld MJ, Kersten SR, Geantet C, Toussaint G, Way NWJ, et al. Hydrodeoxygenation of pyrolysis oil fractions: process understanding and quality assessment through co-processing in refinery units. Energy Environ Sci 2011;4:985–97.
[69] Holmgren J, Marinangeli R, Elliott DC, Bain R. Converting pyrolysis oils to renewable transport fuels: challenges and opportunities. In: NPRA Annual Meeting. , San Diego, United States: UOP LLC; 2008.
[70] Robinson PR, Shaheen EI. Environmental pollution control. In: Hsu CS, Robinson PR, editors. Practical advances in petroleum processing. New York: Springer; 2006. p. 395–447.
[71] Marafi M. Spent catalyst waste minimization and utilization. In: 1st International conference "Hazardous Waste Management", Chania, Crete; 2008.
[72] Liang DT. Management of spent catalysts in petroleum refineries. In: 2nd Asian petroleum technology symposium program, Malaysia. Institute of Environmental Science and Engineering; 2006.
[73] Billege I. 700 Refineries supply oil products to the world. Nafta 2009;60:404–6.
[74] Gerber MA, Frye JG, Bowman LE, Fulton JL, Silva LJ, Wai CM. Regeneration of hydrotreating and FCC catalysts. Washington, United States: Pacific Northwest National Laboratory; 1999.
[75] Marafi M, Stanislaus A, Furimsky E. Environmental and Safety Aspects of Spent Hydroprocessing Catalysts. In: Marafi M, Stanislaus A, Furimsky E, editors. Handbook of Spent Hydroprocessing Catalysts. Elsevier B.V.; 2010. p. 93–120.
[76] Dong C, Zhang Z, Lu Q, Yang Y. Characteristics and mechanism study of analytical fast pyrolysis of poplar wood. Energy Convers Manage 2012;57:49–59.
[77] Oasmaa A, Peacocke C. Properties and fuel use of biomass-derived fast pyrolysis liquids. A guide. VTT Publication 731. Espoo, Finland: VTT Technical Research Centre of Finland; 2010.
[78] Oasmaa A, Solantausta Y, Arpiainen V, Kuoppala E, Sipilä K. Fast pyrolysis bio-oils from wood and agricultural residues. Energ Fuel 2010;24:1380–8.
[79] Guinée JB, Gorrée M, Heijungs R, Huppes G, Kleijn R, de Koning A, et al. Life cycle assessment – An operational guide to the ISO standards. Part 1 – LCA in perspective. Leiden: The Netherlands: Centre of Environmental Science; 2001.
[80] VDI. VDI guideline 4600: Cumulative energy demand (KEA) – Terms, definitions, methods of calculation. Düsseldorf, Germany: Verein Deutscher Ingenieure; 2012.
[81] Goedkoop M, de Schryver A, Oele M, Durksz S, de Roest D. Introduction to LCA with SimaPro 7. Amersfoort, The Netherlands: PRé Consultants; 2010.
[82] EEA. EMEP/EEA air pollutant emission inventory guidebook. Copenhagen, Denmark: European Environment Agency; 2009.